Spatio-temporal modeling of ^{210}Pb transportation in lake environments

Fatih Külahcı [a,*], Zekâi Şen [b]

[a] Firat University, Science and Arts Faculty, Physics Department, Elazığ 23169, Turkey
[b] Istanbul Technical University, Civil Engineering Faculty, Hydraulics and Water Resources Department, Maslak, 34469 Istanbul, Turkey

ARTICLE INFO

ABSTRACT

Radioactive particle movement analysis in any environment gives valuable information about the effects of the concerned environment on the particle and the transportation phenomenon. In this study, the spatio-temporal point cumulative semivariogram (STPCSV) approach is proposed for the analysis of the spatio-temporal changes in the radioactive particle movement within a surface water body. This methodology is applied to the ^{210}Pb radioactive isotope measurements at 44 stations, which are determined beforehand in order to characterize the Keban Dam water environment on the Euphrates River in the southeastern part of Turkey. It considers the contributions coming from all the stations and provides information about the spatio-temporal behavior of ^{210}Pb in the water environment. After having identified the radii of influences at each station it is possible to draw maps for further interpretations. In order to see holistically the spatial changes of the radioisotope after 1st, 3rd and 5th hours, the radius of influence maps are prepared and interpreted accordingly.

© 2008 Elsevier B.V. All rights reserved.

1. Introduction

The spatio-temporal movement of particles in three-dimensional spaces is desirable for particle transportation assessment in different environments such as the atmosphere and hydrosphere. The modeling of such a complicated phenomenon by analytical models needs a set of restrictive assumptions and simplifications, but geostatistical approaches based on field measurements are applicable without restrictions. If the basis of such models is known on scientific philosophical and logical principles with deduction or induction then fruitful descriptions and interpretations can be obtained without much difficulty.

The models built up for the transportation of a particle in aquatic or atmospheric environments are recommended by the researchers in different areas (earth sciences, physics, water resources and environmental engineering). Convenient models are developed for a variety of regional and environmental conditions. For instance, Ng et al. [1] have suggested a numeric model explaining the transportation of the contaminant brought about by the trace elements in the estuaries. Carroll and Harms [2] have concentrated on a hydrodynamic model approach in order to display the uncertainty of the partition coefficient in radionuclide transportation. Additionally, there are spatial and numeric models which help to predict the

position and the quantitative magnitudes of the particles in the atmosphere [3,4].

The first spatial model is performed by Student [5] who summed up the number of the particles per unit area instead of the analysis of the spatial positions of the particles in a liquid. He divided the 1 mm^2 area of a hemacytometer into 400 equal squares, and counted the yeast cells. Later, Fisher [6] used the spatial analysis in agricultural topics. Yates [7] searched about the influence of spatial correlation at the randomization process, where completely random regionalized variables (ReVs) are considered for the modeling purposes.

Matheron [8] suggested geostatistical spatial modeling based on the ReVs, which exposes spatial dependence with distance. The basis of his approach in modeling is the semivariogram (SV) concept where the squared-differences of measurements between any two-measurement sites are considered with the distance, which later become as the Kriging methodology in the literature. This technique is suggested for spatial modeling of the ore grades in mining without time consideration. However, nowadays, the Kriging approach is used in different disciplines provided that there are measurements at a set of irregularly distributed sites in an area.

The studies concerning the spatial modeling of radionuclides do not exist frequently in the literature, however there is steadily increasing trend since the last few years ([9,10]). Especially, spatio-temporal modeling techniques are very rare ([11,12]). On the other hand, the spatio-temporal models for the transportation of the radionuclide are almost non-existent.

* Corresponding author. Tel.: +90 424 2370000/3835; fax: +90 424 2330062.
E-mail address: fatihkulahci@firat.edu.tr (F. Külahcı).

The purpose of this study is to develop a spatio-temporal geo-statistical methodology for modeling the migration of the ^{210}Pb radioisotope in the surface water. The methodology is similar to some previously developed SV, cumulative SV (CSV) and point CSV (PCSV) approaches, which do not take into consideration the time variability. The methodology as suggested in this paper differs from all these SVs by considering also the temporal variability. The application of the suggested methodology is based on a set of samples taken from irregularly distributed locations in the study area, Keban Dam reservoir, Turkey. This approach helps to assess the change of the contribution coming from all of the stations at any desired time. For this purpose, various contour maps are drawn, and the regional behaviors of the radioisotope are examined.

2. Classical variogram methodologies

Let $s \in E^n$ be generic data location in n-dimensional Euclidean space (E^n) and the potential datum $Z(s)$ at spatial location s is a random quantity in the form of a random vector at location $s \in D$, where D is a fixed subset of E^n. Suppose

$$\mathrm{var}(Z(s_1) - Z(s_2)) = 2\gamma(s_1 - s_2), \quad \text{for all } s_1, s_2 \in D \tag{1}$$

Matheron [8] suggested the quantity $2\gamma(\cdot)$, which is a function only of the increment, $s_1 - s_2$, and he named it as a variogram and hence $\gamma(\cdot)$ is a SV [13]. Actually, the concept of SV was used in the scientific literature beforehand as it can be seen in Cressie [14]. It has been called a structure function by Yaglom [15] in the probability context and by Gandin [16] in meteorology, and a mean-squared difference by Jowett [17] in time series. The change with distance on a Cartesian coordinate system of SV is referred to as the SV function, which is explained mathematically as follows by Clark [18].

$$\gamma(d) = \frac{1}{2N_d} \sum_{i=1}^{N_d} (C_i - C_{i+d})^2 \tag{2}$$

where $\gamma(d)$ is the SV value at distance d; C is the radioactive material concentration, and N_d is the total number of equally spaced observations. Various SV alternatives such as the CSV and PCSV are suggested by different researcher [3,19–25].

In the SV concept, it is accepted that the sampling sites in the study area are scattered regularly, yet this may not be the case in actual studies. Besides, as the distance increases, the number of data pairs for calculation of SV decreases, which implies less reliable estimation at large distances. In various disciplines, the sampling positions are irregularly distributed in the region and, therefore, an unbiased estimate of SV is not possible. On the other hand, CSV is defined as the successive summation of half-squared differences which are ranked according to the ascending order of distances extracted from all possible pairs of sample locations within a region. This procedure is useful especially when sampling points are irregularly distributed within the study area. CSV has all the advantages of the classical SV. All of the models that can be formed in SV can also be easily formed with CSV. Neither the SV nor the CSV can explain the regional influences on one point, and they are inadequate in defining quantitative heterogeneity. After CSV, Şen [22] proposed the PCSV technique in order to evaluate the regional heterogeneous behaviors. With the help of this technique, one can observe the contribution of all the stations in the study area on any station. Along the same lines, similar methods have been developed and for instance trigonometric PCSV (TPCSV) technique proposed by Şen and Şahin [26] calculates the radius of influence for any stations.
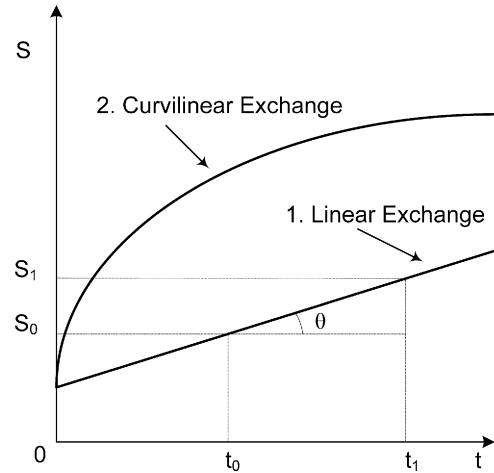

Fig. 1. The change of the linear and curvilinear movement of a particle.

Herein proposed spatio-temporal PCSV (STPCSV) works along the following steps based on the ^{210}Pb radioactivity measurements at a set of irregular sites.

(a) Standardize the available data at distinctive sites by subtraction from each site record, the areal arithmetic average and then by dividing this difference to the areal standard deviation. In this way, ^{210}Pb radioactivity data will be a dimensionless quantity at each station.
(b) Calculate distances between the reference and the remaining sites. If there are n sites the number of distances is $n - 1$, d_j ($j = 1, 2, \ldots, n - 1$).
(c) For each pair calculate the half-squared differences between ^{210}Pb concentrations. Hence, each distance will have corresponding half-squared difference, $0.5(C_i - C_j)^2$, where C_i, and C_j, are the ReVs at the reference and jth sites, respectively.
(d) Plot distances versus corresponding successive cumulative sums of half-squared differences after ranking the distances in ascending order. This procedure will provide a non-decreasing function, which is the sample PCSV at the reference site, i, given by

$$\gamma_i(d) = \frac{1}{2} \sum_{j=1}^{n-1} (Ci - Cj)^2 \tag{3}$$

(e) Apply the previous steps by considering each location as the reference site in turn. Consequently, there are n sample PCSVs obtained from a given set of sites for ^{210}Pb concentration records.

3. Spatio-temporal point cumulative semivariogram

Radioactive particle transportation in any environment is important for detecting the concentration zones spatially and their changes temporally. It is necessary to know the transportation characteristics and the behavior of the particle at later time instances, t, by describing regional movement. In order to be able to define such a movement the following concepts and procedure are suggested based on the classical PCSV. Physically, the particle will have either a linear or non-linear movement on space-time domain as shown in Fig. 1.

Although these movement patterns are shown as continuous lines and curves, in practice, particles move rather randomly, and therefore, continuity in the sense of mathematics is not applicable, but rather statistical averages play role. For instance, in general,
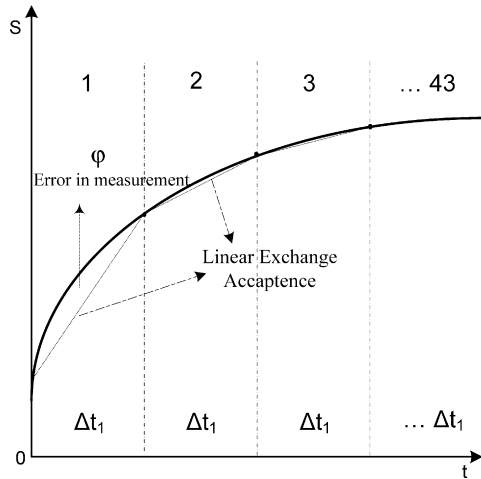
Fig. 2. Piece-wise linear approximations.

^{210}Pb radioisotopes move randomly by the influence of the water waves and turbulence in the lake. However, for the sake of establishing basic concepts, the movement in the space-time domain is considered as continuous.

The slope, θ, of the linear change is the same for all t values and it corresponds to constant velocity as

$$tg\theta = \frac{S_1 - S_0}{t_1 - t_0} \tag{4}$$

where S is the distance. In the non-linear case the slope changes instantaneously in the course of time, where the space variability dependence on time can be expressed in the form of a function as $S = S(t)$. Piece-wise linear approximations are considered as in Fig. 2, where the similar concepts to the linear case can be applicable but with a certain percentage of error, φ. The smaller the segments, the smaller are the error.

This figure is very similar to the classical PCSV, where on the horizontal axis instead of distance time durations are considered. For instance, if there are n number of measurement stations in an area then there will be $(n-1)$ distances from any one of the stations to others. Any station taken as reference will be referred to as the "reference station". Hence, there will be n number of PCSVs for each time instant as

$$\gamma(d_i) = \frac{1}{2} \sum_{j=1}^{n-1} (S_i - S_j)^2 \tag{5}$$

where i is considered as the reference station. By defining $S_i - S_j = \Delta S_{ij}$, it can be rewritten as

$$\gamma(d_i) = \frac{1}{2} \sum_{j=1}^{n-1} (\Delta S_{ij})^2 \tag{6}$$

The velocity of surface water, V, is related to the spatial variability, S, through temporal variability as

$$S = Vt \tag{7}$$

It is assumed that the radioactive components at each station move with the same velocity, and hence, their concentrations, C_j, change by time at station j as CVt, the substitution of which into Eq. (3) leads to the general expression of the STPCSV expression as

$$\gamma(d_i) = \frac{1}{2} \sum_{j=1}^{n} [(CVt)_j - (CVt)_{j-1}]^2 \tag{8}$$

Herein, $(Vt)^2$ can simply be drawn out of the summation, and hence, it plays the role of a scaling factor.

4. Study area and sampling procedures for ^{210}Pb data

Keban Dam Lake is chosen as the study area, which is the second biggest dam in Turkey. There are 44 sample stations in the lake basin of 150 km^2 and surface water samples are taken on April 2007 (Fig. 3). The study area is on the Euphrates River in the eastern Turkey, and it lies at the latitude 38°05′N and longitude 38°04′E. The samples are collected from a depth of nearly 20–30 cm [25,27].

The study area is chosen in such a way that the area-external currents are the least, but Murat Bosporus in the north may cause currents. Murat Bosporus which is at north of research area joins south and north of Dam Lake (Fig. 3). One of the reasons for selecting this area is to analyze the spatial distribution of ^{210}Pb (half-life 22.26 years) in a better manner. Generally, lead may enter the environment during several operations, including mining, ore processing, smelting, refining, manufacture of lead compounds, use of lead metals, alloys and compound in products such as batteries and paints, recycling, and disposal [28]. Furthermore, the measurements are taken when the lake is in its calmest status since the average flow velocity of the water has a vital importance in the STPCSV. Apart from this, the water samples are collected within the same day in order not to be affected by spring rainfalls.

The surface water samples are collected into sterilized clean 2 l polyethylene bottles for subsequent preparation and analyses. An aliquot of 0.5 ml 3N nitric acid is added to prevent the precipitation and absorption of the sample on the container walls. Each sample is divided into three equal parts, and each part is evaporated at low temperature (about 60 °C) until a small amount of water remained. The residue is poured into about 4.6 cm^3 aluminum planchette and dried [29].

In order to determine ^{210}Pb radioactivity, gamma spectrometric is done using a 2″ × 2″ Na(TI) well type detector. It is housed in a cylindrical lead shield of about 13.7 cm and 15.5 cm in diameter and length, respectively. The lead shield thickness is about 3.5 cm and this is suitable for limiting the gamma background. The detector entrance window consists of 0.50 mm thick aluminum. The determination of ^{210}Pb activity concentrations in water sample is based on the detection of 46.50 keV γ rays. The counting time for each sample is 86,000 s [30]. The activity concentrations are calculated according to the following equation:

$$A_{210_{\mathrm{Pb}}}(\mathrm{Bq/l}) = \frac{C}{\xi P_\gamma M_s} \tag{9}$$

where C is the counting rate of γ rays (counts per second), ξ is the detectors efficiency of the specific γ-ray, P_γ is the absolute transition probability of γ-decay and M_S is the mass of the residue in kg or l [29]. The activity values of ^{210}Pb in the lake are given in Table 1.

5. Results and discussion

Before further investigation, it is illuminating to explore the univariate behavior of the data. Hence, the quantile–quantile (Q–Q) plot technique is used for determining whether the two data sets come from the same population or not. A quantile means the fraction (or percent) of points below a given value. For instance, 0.3 (or 30%) quantile is the point below which falls 30% of the data and additionally 45° reference straight-line is also shown in the same figure. If the two sets come from the same population distribution then the points are expected to fall approximately along this straight-line. The greater the departure from it, the greater is the evidence that the two data sets do not come from the same population [31]. The statistical parameters of ^{210}Pb data in Table 1 are
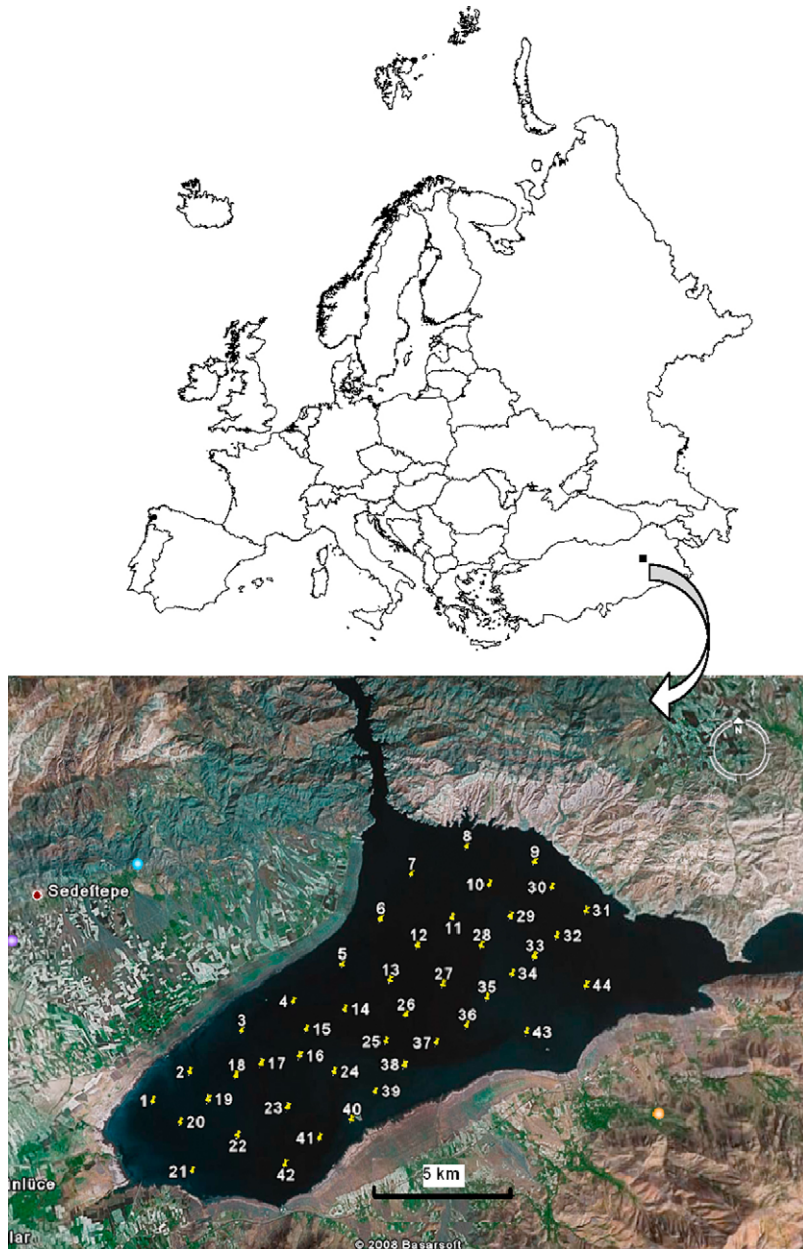
Fig. 3. Study area and station locations.

such that the average is equal to 0.224 Bq/l and the standard deviation is 0.079 Bq/l. The quantile–quantile plot of the data is shown in Fig. 4, where the measurement uncertainty has a median value of coefficient of variation, CV = 0.22.

The logarithmic probability distribution function (PDF) is presented in Fig. 5 for the ^{210}Pb data, which shows a very good correspondence with the theoretical model. The theoretical logarithmic PDF, $f(x)$ of x variable is given by the following expression, where μ and σ are the logarithmic mean and standard deviation, respectively:

$$f(x) = \frac{1}{x\sigma\sqrt{2\pi}} e^{-1/2((\log(x-\mu)/\sigma)^2} \qquad (10)$$

Furthermore, based on the coordinates given in Table 1, the experimental SV can be modeled after the removal of linear drift as spherical function with range equal to 3110 m; nugget effect as 0.00173 (Bq/l)^2; scale 0.004 (Bq/l)^2; anisotropy ratio 2; main axis
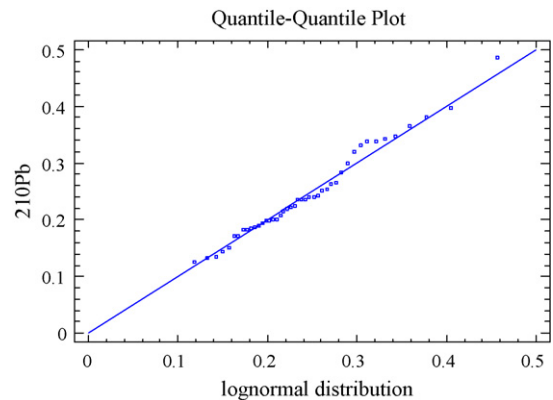

Fig. 4. Q–Q plot of ^{210}Pb concentrations.

Table 1
Locations of stations and ^{210}Pb radioactivity concentrations.

| Station	Latitude (N)	Longitude (E)	[210]Pb (Bq/l)
1	38.3722	39.2419	0.133 ± 0.044
2	38.3752	39.2452	0.235 ± 0.114
3	38.3832	39.2553	0.134 ± 0.098
4	38.3859	39.2658	0.126 ± 0.021
5	38.3927	39.2800	0.172 ± 0.149
6	38.4012	39.2850	0.338 ± 0.081
7	38.4048	39.2924	0.252 ± 0.016
8	38.4112	39.3034	0.172 ± 0.051
9	38.4053	39.3158	0.199 ± 0.050
10	38.4032	39.3058	0.208 ± 0.072
11	38.4008	39.3017	0.263 ± 0.021
12	38.3941	39.2937	0.236 ± 0.079
13	38.3910	39.2857	0.150 ± 0.086
14	38.3839	39.2800	0.396 ± 0.210
15	38.3824	39.2713	0.319 ± 0.104
16	38.3759	39.2740	0.338 ± 0.194
17	38.3754	39.2618	0.145 ± 0.010
18	38.3744	39.2547	0.264 ± 0.104
19	38.3723	39.2513	0.194 ± 0.025
20	38.3711	39.2437	0.223 ± 0.027
21	38.3617	39.2450	0.365 ± 0.140
22	38.3648	39.2545	0.201 ± 0.020
23	38.3712	39.2647	0.184 ± 0.019
24	38.3743	39.2744	0.347 ± 0.053
25	38.3811	39.2846	0.190 ± 0.054
26	38.3833	39.2912	0.236 ± 0.047
27	38.3902	39.2957	0.282 ± 0.063
28	38.3933	39.3046	0.222 ± 0.025
29	38.3959	39.3123	0.243 ± 0.029
30	38.4024	39.3213	0.198 ± 0.048
31	38.4000	39.3253	0.219 ± 0.052
32	38.3938	39.3217	0.187 ± 0.040
33	38.3921	39.3149	0.183 ± 0.051
34	38.3906	39.3121	0.200 ± 0.045
35	38.3845	39.3050	0.330 ± 0.046
36	38.3820	39.3024	0.381 ± 0.040
37	38.3808	39.2947	0.240 ± 0.039
38	38.3751	39.2908	0.343 ± 0.065
39	38.3723	39.2832	0.253 ± 0.069
40	38.3658	39.2820	0.486 ± 0.345
41	38.3647	39.2720	0.214 ± 0.038
42	38.3619	39.2640	0.239 ± 0.052
43	38.3811	39.3135	0.298 ± 0.049
44	38.3851	39.3249	0.183 ± 0.041
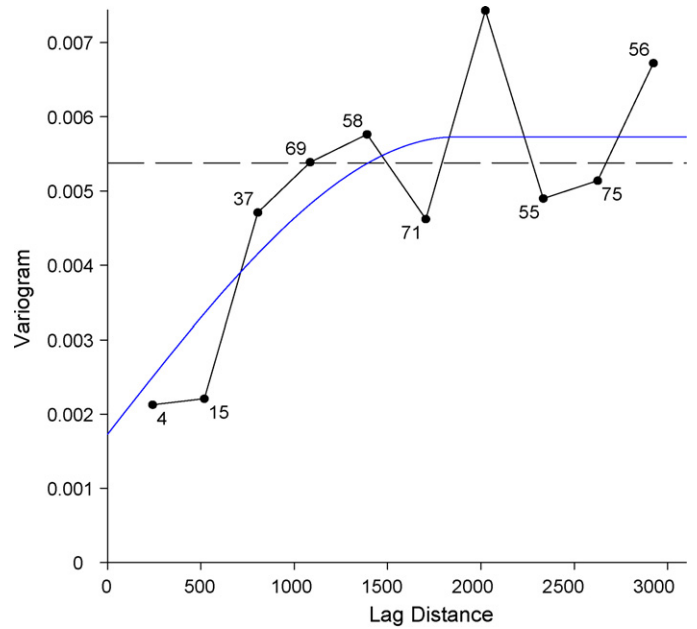
Fig. 6. Experimental SV and theoretical spherical model.

projection as 120° (see Fig. 6). The SV of the log data has an estimated nugget of 0.04, which through nug(log) ≈ CV² = 0.048 shows that the nugget is mainly due to data noise, with probably only minor spatial micro-variance component. Given this likely physical smoothness of the data, also the assumption of a Gaussian variogram is justified. Based on these values, it is possible to obtain ^{210}Pb concentration (Bq/l) map as in Fig. 7. It is obvious from this map that the anisotropy is well visible, includes essentially all the information that can be derived from the data presented in Table 1. For a physical interpretation the local hydrological conditions must be known.

The concentrations, C, for the application of Eq. (8) are given in Table 1. The velocities of surface water (V) for 44 stations are
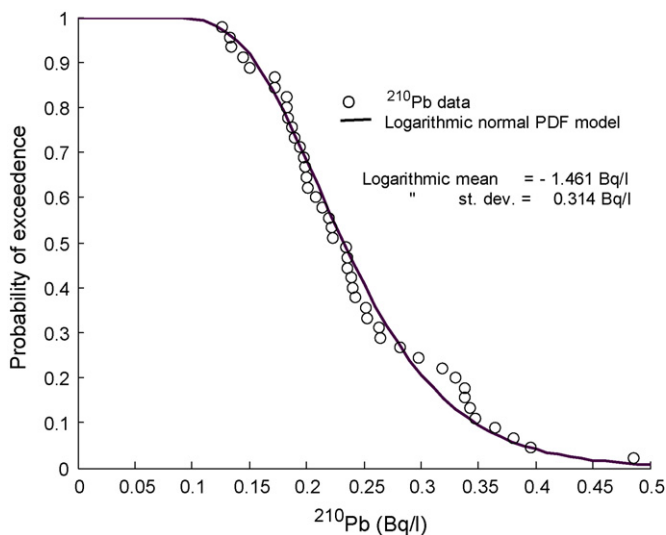

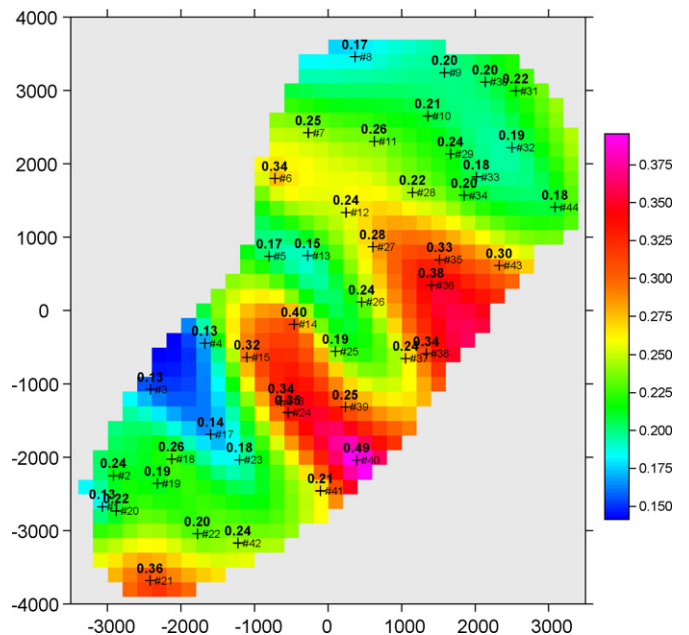**Fig. 5.** Logarithmic normal PDF model for ^{210}Pb data.

Fig. 7. [210]Pb concentration map (Bq/l).

calculated with "velocity measurement guide". This simple guide consists of a chronometer, fishing line and mechanism which can swim upper water. The velocity measurement process for every station is repeated three times and it is shown in Fig. 8. This calculation is performed within the same day, in 24 h. First the application of Eq. (3) in the form of the classical PCSV is performed for Keban Dam measurement stations and the results are presented in Fig. 8. This can be considered as a special STPCSV provided that $t = 1$ h.

In order to be able to see clearly the temporal analysis of STPCSV on the whole area, for each station the radius of influence is determined in terms of radioactivity variable in a single STPCSV graph. As in Fig. 9a, a model is fitted to data by using the least squares method, and the radius of influence corresponds to the distance in which the change continues until it becomes a linear function. The distance, d, on the horizontal axis corresponding to a fixed magnitude change, M, is the radius of influence at that station, and it can be expressed mathematically as

$$\lim_{d_i \to \infty} \frac{\partial \gamma(d)}{\partial d} = M \qquad (11)$$

The maps obtained by classical SV methods can only give stationary information, since there is no time change [14]. Neither the CSV nor the PCSV can analyze the time variability even though it is possible to inquire spatial variability. In this study, there are 44 STPCSV graphs corresponding to 44 stations given in Table 1. Moreover, these STPCSV changes of ^{210}Pb are examined in the 1st, 3rd and 5th hours. Fig. 9b presents the STPCSV graph for 10th station where the structural change of ^{210}Pb can be observed clearly as time passes. This figure indicates that the trace of the scatter points do not pass from the origin, which displays that ^{210}Pb is not affected by the geological, geographical, etc. characteristics of the environment. If PCSV and STPCSV intersect the vertical axis, there is then a nugget effect in the regional variability of ^{210}Pb. The similar interpretations are possible separately for each one of the 44 stations. Due to space limitation, it is not possible to expose them all. After having obtained the radius of influence for each station then the map of radii of influences give detailed spatio-temporal information in terms of the concerned variable in a set of time segments as defined above.
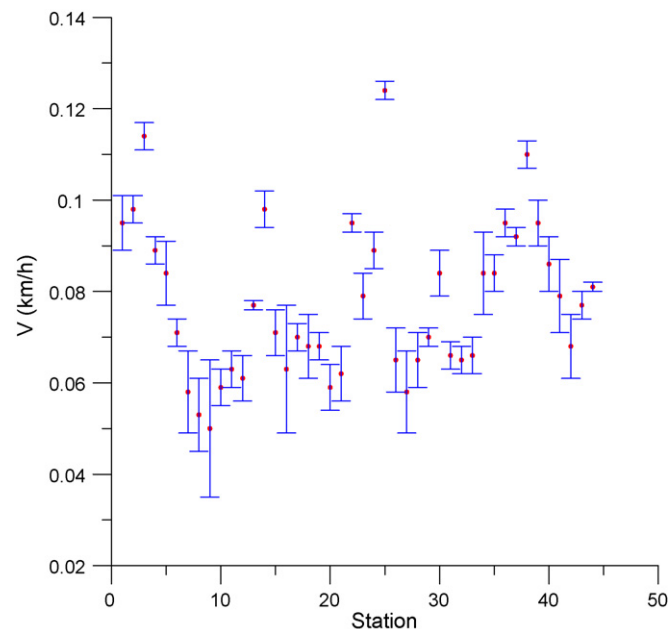

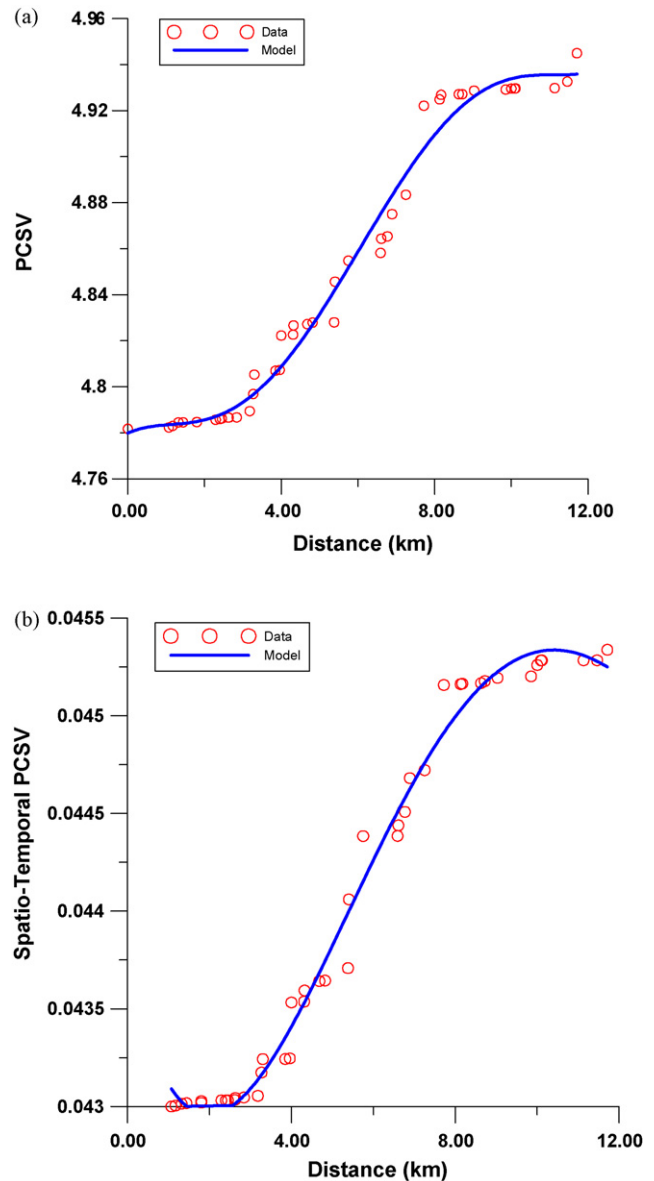**Fig. 8.** Velocities of surface water of stations.

Fig. 9. (a) Sample PCSV; (b) STPCSV graph for 10th station.

After the common interpretations about the 10th station, the intersection point on the vertical axis moves away from the origin together with the advance in time in STPCSV graphs. This divergence shows that the regional diversities of ^{210}Pb should also increase as time advances.

6. Spatio-temporal maps

It is possible to see the spatio-temporal distribution of ^{210}Pb in detail on the radius of influence maps based on STPCSVs (Fig. 10). These maps are drawn by making use of Golden Software programme [32] and Kriging's method [13]. On the same figure, the spatial changes of ^{210}Pb at 1st, 3rd and 5th hours are drawn by considering the radius of influence for $r = 1$ km and 3 km. Due to the rareness of wave movements in the lake, it is feasible to conduct a holistic analysis in terms of space-time. Hence, it is possible to appreciate the minor chances from these maps.

It is seen that the frequency of the identical curves diminishes to a small extent when the radius of influence moves from $r = 1$ km to
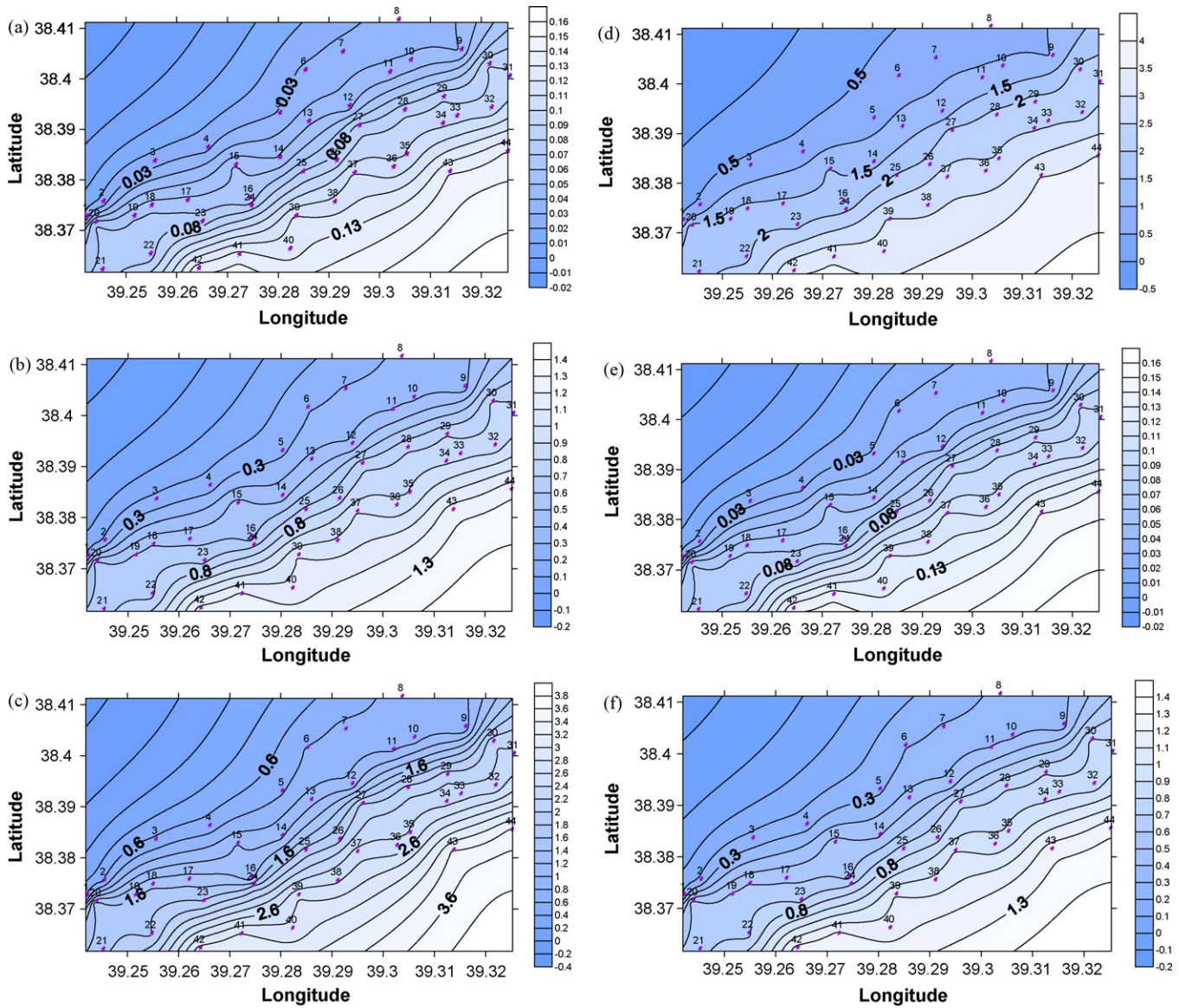
Fig. 10. (a) Radius of influence for 1 km at 1 h. (b) Radius of influence for 1 km at 3 h. (c) Radius of influence for 1 km at 5 h. (d) Radius of influence for 3 km at 5 h. (e) Radius of influence for 3 km at 1 h. (f) Radius of influence for 3 km at 3 h.

3 km. This is also valid for the situation when the duration increases (Fig. 10c and d).

As it is seen in Fig. 10b–f at the lake's middle section, there are high similarities, which can connect dominant currents at the lake's middle section. At $t = 1$ h, the changes of $r = 1$ km and 3 km show big similarities. The changes of radioactivity at $r = 3$ km have bigger similarities. This change can be explained as the time passes, the radioactivity mixture takes a homogenous state. After long times, homogenous state is an expected result in radioactivity concentrations. As a matter of fact, this situation is clearly seen in Fig. 10d according to other iso-maps, where the density diminishes and there is an increase in the similarity. [210]Pb concentration temporal change is presented in Fig. 10d.

7. Conclusions

For the spatio-temporal analysis of radioactive isotope transportation spatio-temporal point cumulative semivariogram method is developed and applied to ^{210}Pb concentrations in the Keban Dam reservoir in the southeastern province of Turkey. It is observed that different interpretations can be acquired from STPCSVs. Additionally, it forms a temporal analysis as well as supports the information gained from the classical cumulative semivariogram and point CSV. It is possible to apply STPCSV methodology easily to particle movement in rivers, oceans or in atmosphere apart from systems like dam lakes. Among such phenomena are the nuclear wastes' distributions in environment, fallouts, atmospheric contaminations or other meteorological applications, the distribution of the heavy metal, etc.

In order to attain maximum reliability in similar studies, the credibility of STPCSV will increase by using as many stations as possible. The radius of influence of each station can be calculated for a set of desired hours and their maps help to make regional interpretations concerning the spatio-temporal radioactivity variation in the lake.

STPCSV shows that as long as the time passes change, of the radioactivity concentrations in lake takes a homogenous state.

Acknowledgements

References

[1] B. Ng, A. Turner, A.O. Tyler, R.A. Falconer, G.E. Millward, Modelling contaminant geochemistry in estuaries, Water Res. 30 (1996) 63–74.

[2] J. Carroll, I.H. Harms, Uncertainty analysis of partition coefficients in a radionuclide transport model, Water Res. 33 (1999) 2617–2626.

[3] Z. Şen, An application of a regional air pollution estimation model over Istanbul urban area, Atmos. Environ. 32 (1998) 3425–3433.

[4] L.M. Frohn, J.H. Christensen, J. Brandt, Development of a high-resolution nested air pollution model: the numerical approach, J. Comput. Phys. 179 (2002) 68–94.

[5] Student, On the error of counting with a hemacytometer, Biometrika 5 (1907) 351–360.

[6] R.A. Fisher, The Design of Experiments, Oliver and Boyd, Edinburgh, 1935.

[7] F. Yates, The comparative advantages of systematic and randomized arrangements in the design of agricultural and biological experiments, Biometrika 30 (1938) 444–466.

[8] G. Matheron, Principles of geostatistics, Econ. Geol. 58 (1963) 1246–1266.

[9] H.S. Viswanathan, B.A. Robinson, C.W. Gable, J.W. Carey, A geostatistical modeling study of the effect of heterogeneity on radionuclide transport in the unsaturated zone, Yucca Mountain, J. Contam. Hydrol. 62 (2003) 319–336.

[10] G. Severino, V. Cvetkovic, A. Coppola, Spatial moments for colloid-enhanced radionuclide transport in heterogeneous aquifers, Adv. Water Resour. 30 (2007) 101–112.

[11] S.J. Deutsch, P.E. Preiffer, Space-time ARMA modelling with contemporaneously correlated innovations, Technometrics 23 (1981) 401–409.

[12] R.A. Bilonick, The space-time distribution of sulfate deposition in the northeastern United States, Atmos. Environ. 19 (1985) 1829–1845.

[13] N.A.C. Cressie, Statistics for Spatial Data, John Wiley & Sons Inc., New York, 1991, 900 pp.

[14] N.A.C. Cressie, in: S. Kotz, N.L. Johnson (Eds.), Variogram, entry in encyclopedia of statistical sciences, vol. 9, Wiley, New York, 1988, pp. 489–491.

[15] A.M. Yaglom, Some classes of random fields in *n*-dimensional space, related to stationary random processes, Theor. Probab. Appl. 2 (1957) 273–320.

[16] L.S. Gandin, Objective analysis of meteorological fields, Gidrometeorologicheskoe izdatel'stvo (GIMIZ), Leningrad (Translated, Jerusalem, 1965), 1963.

[17] G.H. Jowett, The accuracy of systematic sampling from conveyer belts, Appl. Stat. 1 (1952) 50–59.

[18] I. Clark, The semivariogram-Part 1, J. Eng. Min. 7 (1979) 90–94.

[19] Z. Şen, Cumulative semivariogram models of regionalized variables, Int. J. Math. Geol. 21 (1989) 891–903.

[20] Z. Şen, Standard cumulative semivariograms of stationary stochastic processes and regional correlation, Int. J. Math. Geol. 24 (1991) 417–435.

[21] Z. Şen, Objective analysis of cumulative semivariogram technique and its application in Turkey, J. Appl. Meteorol. 36 (1997) 1712–1720.

[22] Z. Şen, Point cumulative semivariogram for identification of heterogeneities in Regional Seismicity of Turkey, Int. J. Math. Geol. 30 (1998) 767–787.

[23] Z. Şen, A.D. Şahin, Regional assessment of wind power in western Turkey by the cumulative semivariogram method, Renew. Energy 12 (1997) 169–177.

[24] Z. Şen, Z. Habib, Point cumulative semivariogram of areal precipitation in mountainous region, J. Hydrol. 205 (1998) 81–91.

[25] F. Külahcı, Z. Şen, Spatial dispersion modeling of ^{90}Sr by point cumulative semivariogram at Keban Dam Lake, Turkey, Appl. Radiat. Isot. 65 (2007) 1070–1077.

[26] Z. Şen, A.D. Şahin, A new spatial prediction model and its application to wind records, Theor. Appl. Climatol. 79 (2004) 45–54.

[27] F. Külahcı, Z. Şen, Perturbation distribution coefficient definition, Fresenius Environ. Bull. 17 (3) (2008) 326–330.

[28] E. Merian, M. Anke, M. Ihnat, M. Stoeppler, Elements and Their Compounds in the Environment, vol. 2, John Wiley, Weinheim, 2004, 1455 pp.

[29] F. Külahcı, Z. Şen, Multivariate statistical analyses of artificial radionuclides and heavy metals contaminations in deep mud of Keban Dam Lake, Turkey, Appl. Radiat. Isot. 66 (2008) 236–246.

[30] D.E. Walling, Q. He, Using fallout lead-210 measurements to estimate soil erosion on cultivated land, Soil Sci. Soc. Am. J. 63 (1999) 1404–1412.

[31] NIST/SEMATECH, e-Handbook of Statistical Methods, 2008, http://www.itl.nist.gov/div898/handbook.

[32] Golden Software, Golden Software, Surfer 7.0, Contouring and 3D Surface Mapping for Scientists and Engineers, User's Guide, Golden Software Inc., 1999, 640 pp.